

THE ACTIVE FRACTURE MODEL: ITS RELATION TO FRACTAL FLOW PATTERNS AND A FURTHER EVALUATION USING FIELD OBSERVATIONS

H.H. Liu, G. Zhang and G.S. Bodvarsson

Earth Sciences Division
LBNL
Berkeley, CA 94720, USA
e-mail: hhliu@lbl.gov

ABSTRACT

The active fracture model (AFM) has been used in modeling flow and transport in the unsaturated zone of Yucca Mountain, Nevada, a proposed repository of high-level nuclear waste. This study presents an in-depth evaluation of the AFM, based on both theoretical arguments and field observations. We first argue that flow patterns observed from different unsaturated systems (including the unsaturated zone of Yucca Mountain) may be fractals. We derive a closed-form relation between the AFM and the fractal flow behavior, indicating that the AFM essentially captures this important flow behavior at a subgrid scale. Finally, the validity of the AFM is demonstrated by the favorable comparison between simulation results based on the AFM and C-14 age and fracture coating data collected from the unsaturated zone at Yucca Mountain. These data sets independently provide important insight into flow and transport processes at the Yucca Mountain site.

INTRODUCTION

Flow and transport in unsaturated fractured rocks are generally complicated because of the complexity of fracture-matrix interaction mechanisms, distinct differences in hydraulic properties between fractures and the matrix, and nonlinearity involved in unsaturated flow. Recently, the investigation into using the unsaturated zone at Yucca Mountain, Nevada, as a proposed storage facility for the geological disposal of high-level nuclear wastes has generated intensive research interests in modeling flow and transport in unsaturated fractured rocks (e.g., Bodvarsson and Tsang, 1999). Modeling flow and transport in unsaturated fractured rocks is also of interest in other areas including environmental contamination in arid and semiarid regions.

Continuum approaches are commonly used for modeling flow and transport in unsaturated fractured rocks. A traditional continuum approach assumes uniformly distributed flow patterns at a subgrid scale and therefore cannot be used for representing gravity-driven fingering flow and transport in fracture networks, resulting from subsurface heterogeneities and nonlinearity involved in unsaturated flow (e.g., Glass et al., 1996; Liu et al., 1998; Su et al., 1999;

Pruess et al., 1999). In an effort to incorporate this flow behavior into the continuum approach, Liu et al. (1998) developed an active fracture model (AFM) that assumes only a portion of fractures in a connected unsaturated fracture network to contribute to liquid water flow. While previous studies have shown that simulation results based on the AFM are generally consistent with field observations from the unsaturated zone of Yucca Mountain (Liu et al., 1998), the major objective of this work is to provide a further evaluation of the AFM, based on both theoretical arguments and field observations.

ACTIVE FRACTURE MODEL

The AFM was developed within the context of the dual-continuum approach (Liu et al., 1998). While the details of the AFM can be found in Liu et al. (1998), a brief introduction of the AFM is provided here for convenience. The active fracture concept is based on the reasoning that, because of the fingering flow, only a portion of fractures in a connected, unsaturated fracture network contribute to liquid water flow, while other fractures are simply bypassed. The portion of the connected fractures that actively conduct water are called active fractures.

Flow and transport conditions and fractured rock properties should determine the fraction of active fractures in a connected fracture network, f_a . An expression for f_a must satisfy the following conditions: all connected fractures are active ($f_a = 1$) if the system is fully liquid saturated; all fractures are inactive ($f_a = 0$) if the system is at residual saturation; and f_a should be related to water flux in fractures. It is generally believed that more fractures are conducive to a larger water flux. This water flux in fractures is considered to be mainly dependent on fracture saturation because fracture water flow is gravity-dominated. A simple expression for $f_a(-)$, which meets these conditions and includes only one parameter, is a power function of effective water saturation in connected fractures, $S_e(-)$:

$$f_a = S_e^\gamma \quad (1)$$

where $\gamma (-)$ is a positive constant depending on properties of the corresponding fracture network, and

the effective water saturation in connected fractures is given by

$$S_e = \frac{S_f - S_r}{1 - S_r} \quad (2)$$

where $S_f(-)$ is the water saturation of all connected fractures and S_r is the residual fracture saturation. In this study, Eq. (1) is used to determine the fraction of active fractures. As will be discussed below, this simple equation is actually the first-order approximation for fractal flow behavior at a subgrid scale.

Note that only the active fracture continuum, a portion of the total fracture continuum, contributes to flow and transport in fractures and fracture-matrix interaction. Fracture hydraulic properties should thus be defined for active fractures. The effective water saturation of active fractures, $S_{ac}(-)$, is related to the effective water saturation in connected fractures, S_e , by

$$S_{ac} = \frac{S_e}{f_a} = S_e^{1-\gamma} \quad (3)$$

Because $S_{ac} \leq 1$, γ should be smaller than or equal to one. The effective water saturation of active fractures is related to the actual water saturation in active fractures, S_a , by

$$S_{ac} = \frac{S_a - S_r}{1 - S_r} \quad (4)$$

The well-known van Genuchten (1980) relation is used in the current version of the AFM for describing constitutive relationships for the active fracture continuum (Liu et al., 1998).

In summary, the active fracture model uses a combination of the volume-averaged method and a simple filter to deal with fracture flow and transport. Inactive fractures are filtered out in modeling fracture-matrix interaction, flow, and transport in the fracture continuum. The γ factor may be interpreted as a measure of the “activity” of connected fractures. Generally speaking, a smaller γ value corresponds to a larger number of active fractures in a connected fracture network. For example, $\gamma = 0$ results in all connected fractures being active. On the other hand, $\gamma = 1$ corresponds to zero fracture capillary pressure, indicating that all active fractures are saturated.

THE AFM AND FRACTAL FLOW BEHAVIOR IN UNSATURATED SYSTEMS

A flow system exhibits so-called fractal flow behavior when the corresponding flow patterns can be characterized by fractals. In this section, a brief discussion of fractal dimension (used for characterizing fractal patterns) is presented, followed

by a discussion of evidence for fractal flow behavior in unsaturated systems and relations between the AFM and this fractal flow behavior.

Fractal Dimension

Fractal dimension, d_f , is generally a noninteger and less than the corresponding Euclidean (topological) dimension of a space, D . Different kinds of definitions of fractal dimension exist. The most straightforward definition is the so-called box dimension, based on a simple “box-counting” procedure. This dimension is determined from Eq. (5) (below) by counting the number (N) of “boxes” (e.g., line segment, square and cubic for one-, two-, and three-dimensional problems, respectively), needed to cover a spatial pattern, as a function of the box size (l) (e.g., Feder, 1988):

$$N(l) = \left(\frac{L}{l}\right)^{d_f} \quad (5)$$

where L refers to the size of the entire spatial domain under consideration (Fig. 1).

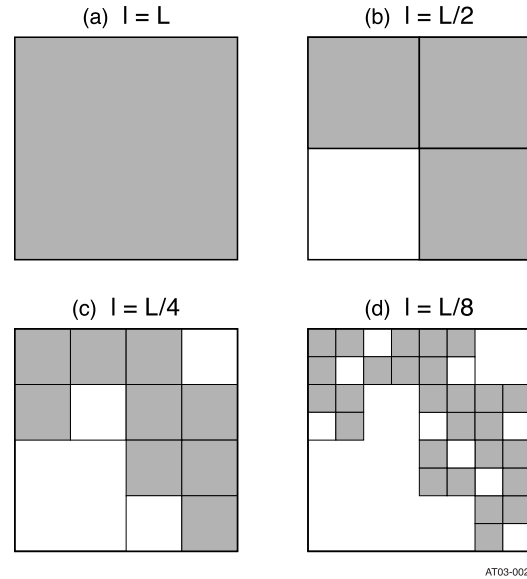


Figure 1. Demonstration of the “box” counting procedure for several box sizes

Obviously, if a spatial pattern is uniformly distributed in space, the fractal dimension will be identical to the corresponding Euclidean dimension. In this case, the box number, N^* , and the box size l have the following relation

$$N^*(l) = \left(\frac{L}{l}\right)^D \quad (6)$$

A fractal pattern exhibits similarity at different scales. When $d_f < D$, the corresponding pattern does not fill the whole space, but only part of it (Fig. 1).

Fractal Flow Behavior in Unsaturated Systems

Fractals have been shown to provide a common language for describing many different natural and social phenomena (Mandelbrot, 1982). While a vast literature exists on the validity of the fractal concept for a great number of fields, fractals have been found to be useful for representing many spatial distributions in subsurface hydrology, including complex flow (or solute transport) patterns in unsaturated systems.

Flury and Flühler (1995) first indicated that solute leaching patterns, observed from three field plots consisting of an unsaturated loamy soil, could be well represented by a diffusion-limited aggregation (DLA) model (Witten and Sander, 1981), although the relation between DLA parameters and soil hydraulic properties is still an unresolved issue. It has been documented that DLA generates fractal patterns (e.g., Feder, 1988; Flury and Flühler, 1995). The observation of Flury and Flühler (1995) is further supported by a study of Persson et al. (2001), who used dye-infiltration data to investigate field pathways of water and solutes under unsaturated conditions. Persson et al. (2001) showed that field observations are well described by the DLA model. Furthermore, they demonstrated that observed mean power spectrum for dye penetration of a field plot displays a typical power-law relationship, another important indication of fractal flow behavior. Glass (1993) first showed that unsaturated flow in a single vertical fracture is characterized by gravity-driven fingers, and the resulting flow patterns could be modeled by an invasion-percolation approach (Wilkinson and Wilemsen, 1983). Again, percolation-based models generate fractal clustering patterns (Stauffer and Aharony, 2001). Closely related to flow and transport processes in unsaturated systems, flow patterns observed from multiphase systems are also related to fractals. For example, viscous fingering in porous media has been experimentally shown to be fractal (Feder, 1988). The problem of viscous fingering in porous media is of central importance in oil recovery. Smith and Zhang (2001) also reported that DNAPL fingering in water saturated porous media, observed from sandbox experiments, is fractal.

Detailed experimental studies on unsaturated flow patterns in large-scale fracture networks are scarce in the literature, because of the technical difficulties in observing these patterns in the field. Fortunately, some geochemical data sets closely related to flow patterns in large-scale fracture networks have recently become available from the unsaturated zone of Yucca Mountain. For example, a spatial distribution of fractures with mineral coatings was determined along an underground tunnel, using a detailed-line-survey method (Paces et al., 1996). The

total survey length along the tunnel is several thousand meters, broken up by a number of disconnected 30 m survey intervals. As will be discussed below, fracture coating is roughly a signature of water flow paths. Therefore, this data set can be used to infer potential fractal flow behavior at a large fracture-network scale.

The intersections of coated fractures with the survey line (along the underground tunnel) form a set of points. If the corresponding flow pattern is fractal, the point set should be fractal too. A box-counting method is used to detect the fractal pattern from this point set. Fig. 2 shows number of boxes (line segments), N , covering at least one intersection point as a function of box size (length of a segment), l . Note that the largest box size corresponds to the length of survey intervals (30 m). The smallest box size used here is 3 m. If all fractures are coated, all boxes of this size or larger should at least cover one of the intersection points, because the average fracture spacing is much smaller than this size. This corresponds to a dimension of one (the topological dimension) based on Eq. (6).

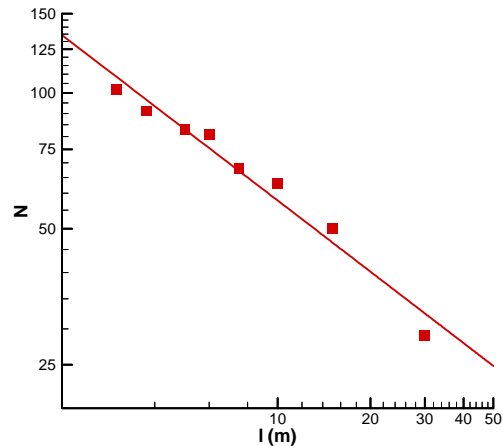


Figure 2. Relation between the number of box (N), covering at least one intersection between coated fractures and the survey line, as a function of box size l .

Fig. 2 shows that the data points can be fitted by a power function with a power of -0.5 , indicating the existence of a fractal pattern for coated fractures (or flow paths). The power value suggests a fractal dimension of 0.5 that is not an integer but smaller than the corresponding topological dimension (one).

A Relation between the AFM and Fractal Flow Patterns

We have shown that flow processes in unsaturated systems (including fracture networks) may be fractal. This has many important implications regarding the development of numerical models for large-scale unsaturated systems, because fractal patterns are

generally related to fingering and/or preferential flow paths. In this section, we will demonstrate the AFM's consistency with fractal flow behavior in unsaturated fracture networks.

Consider Fig. 1(a) to be a gridblock containing a fracture network and the corresponding flow pattern in the fracture network to be fractal. In this case, only a portion of the medium within a gridblock contributes to water flow (Fig. 1). This is conceptually consistent with the AFM (Liu et al. 1998). Note that in Fig. 1, a box is shadowed if it covers one or more fractures (or fracture segments) that conduct water. For simplicity, further consider that fractures are randomly distributed in space, and thus the dimension for water-saturation distribution is the corresponding Euclidean dimension when all the connected fractures actively conduct water. As will be obvious from the derivations to follow, this assumption does not alter our general conclusion regarding the connection between the AFM and fractal flow patterns.

Combining Eqs. (5) and (6) yields

$$[N(l)]^{1/d_f} = [N^*(l)]^{1/D} \quad (7)$$

The average water saturation (S_e) for the whole gridblock (Fig. 1(a)) is determined to be

$$S_e = \frac{V}{l^D \phi N^*(l)} \quad (8)$$

where V is the total water volume (excluding residual water) in fractures within the gridblock (Fig. 1a), and ϕ is fracture porosity. Similarly, the average water saturation (S_b) for shadowed boxes with a size of l is

$$S_b = \frac{V}{l^D \phi N(l)} \quad (9)$$

From Fig. 1, it is obvious that there exists a box size $l_1 < L$ satisfying:

$$\frac{V}{l_1^D \phi} = 1 \quad (10)$$

Based on Eqs. (7)–(10), the average saturation for shadowed boxes with size l , S_{b1} , can be expressed by

$$S_{b1} = (S_e)^{\frac{d_f}{D}} \quad (11)$$

Because a fractal is similar at different scales, the procedure to derive Eq. (11) from a gridblock with size L can be applied to shadowed boxes with the smaller size of l . In this case, for a given box size smaller than l_1 , the number of shadowed boxes will be counted as an average number for those within the

(previously shadowed) boxes with a size of l_1 . Again, we can find a box size $l_2 < l_1$ to obtain a saturation relation:

$$S_{b2} = (S_{b1})^{\frac{d_f}{D}} = (S_e)^{\left(\frac{d_f}{D}\right)^2} \quad (12)$$

The procedure to obtain Eq. (12) can be continued until it reaches an iteration level, n^* , at which all the shadowed boxes with a size of l_n cover active fractures only. The resultant average saturation for these shadowed boxes is

$$S_{bn} = (S_e)^{\left(\frac{d_f}{D}\right)^{n^*}} \quad (13)$$

By definition of active fractures, S_{bn} should be equivalent to the effective saturation of active fractures. It is remarkable that Eq. (13) is similar to Eq. (3), obtained from a key hypothesis of the AFM that the fraction of active fractures in an unsaturated fracture network is a power function of the average effective saturation of the network. Comparing these two equations yields

$$\gamma = 1 - \left(\frac{d_f}{D}\right)^{n^*} \quad (14)$$

Eq. (14) provides the first theoretical relation between the AFM parameter γ and the fractal dimension, while γ was initially developed as an empirical parameter (Liu et al., 1998). Thus, the AFM essentially captures fractal flow behavior at the gridblock scale ($d_f < D$), whereas traditional continuum approaches assume a uniform flow pattern (or effective-saturation distribution) at that scale (corresponding to $d_f = D$ or $\gamma = 0$). In other words, the AFM can be used for simulating fractal flow behavior (in an unsaturated fracture network) that cannot be handled by traditional continuum approaches.

EVALUATION OF THE AFM USING FIELD OBSERVATIONS

So far, we have shown that fractal flow behavior may be common in different unsaturated systems (including unsaturated fracture networks) and also that the AFM is, in general, consistent with this behavior. In this section, we will further evaluate the AFM using different data sets collected from the Yucca Mountain site. Considering the complexity of large-scale unsaturated flow and transport in fractured porous media, the direct use of actual field data for evaluating a model is critical. In this study, we focus on evaluating the AFM with C-14 age data and fracture coating data that provide important information regarding large-scale unsaturated flow processes in fractures and fracture-matrix interaction.

C-14 and Fracture Coating Data

Carbon-14 data have been collected from perched water, pore water, and gas samples from the unsaturated zone of Yucca Mountain (Yang, 2002). Carbon-14 data from gas samples are most representative of *in situ* conditions (Yang, 2002). The determined carbon-14 residual ages from these gas samples are considered to be the same as ages of the *in situ* pore water because of the local equilibrium, as suggested by Yang (2002).

The process of unsaturated-zone mineral deposition is initiated during infiltration where meteoric water interacts with materials in the soil, after which a portion may then enter the bedrock fracture network. Fracture coating is generally a signature of water flow paths. Thus, the coating data are useful for validating the AFM that describes water flow in fractures. Fracture coating data were collected in an underground tunnel in the unsaturated zone of Yucca Mountain. Observed spatial distribution of fractures with coatings is used to estimate the portion of active fractures (about 10%). Mineral-coating growth rate data imply that the unsaturated zone fracture network has maintained a large degree of hydrologic stability over time, and that fracture flow paths in the deep unsaturated zone are buffered from climate-induced variations in precipitation and infiltration (Fabryka-Martin et al., 2000).

Comparison between Simulation Results and Field Observations

One-dimensional dual-permeability numerical models are developed for boreholes USW SD-12 and USW UZ-1 where C-14 data were collected. Calibrated rock properties (Liu and Ahlers, 2003) are used, except for γ values associated with the TSw formation, where the repository is proposed to be located. The value of the AFM parameter γ for the TSw formation is varied for different simulations to check the sensitivity of simulated water travel times to this parameter within the formation. The top boundary condition corresponds to the present-day infiltration rate for flow simulations and a constant tracer concentration for transport simulations. The initial condition for solute transport is zero concentration within the fractured rocks. Previous studies indicate that dispersion processes have an insignificant effect on overall solute transport behavior in unsaturated fractured rocks (Bodvarsson et al., 2000), and therefore are ignored here. An effective-diffusion-coefficient value of $1.97E-10$ m²/s is employed, which is equal to the average value of coefficients for tritiated water measured from tuff matrix samples. TOUGH2 and T2R3D codes (Pruess, 1991; Wu et al., 1996) are used for simulating steady-state water flow and tracer transport processes. Simulated water travel times (or ages) for rock matrix

are compared with carbon-14 ages. A simulated water travel time at a location is determined as the time when the matrix concentration reaches 50% of the top-boundary concentration. It represents the average travel time for water particles from the ground surface to the location under consideration.

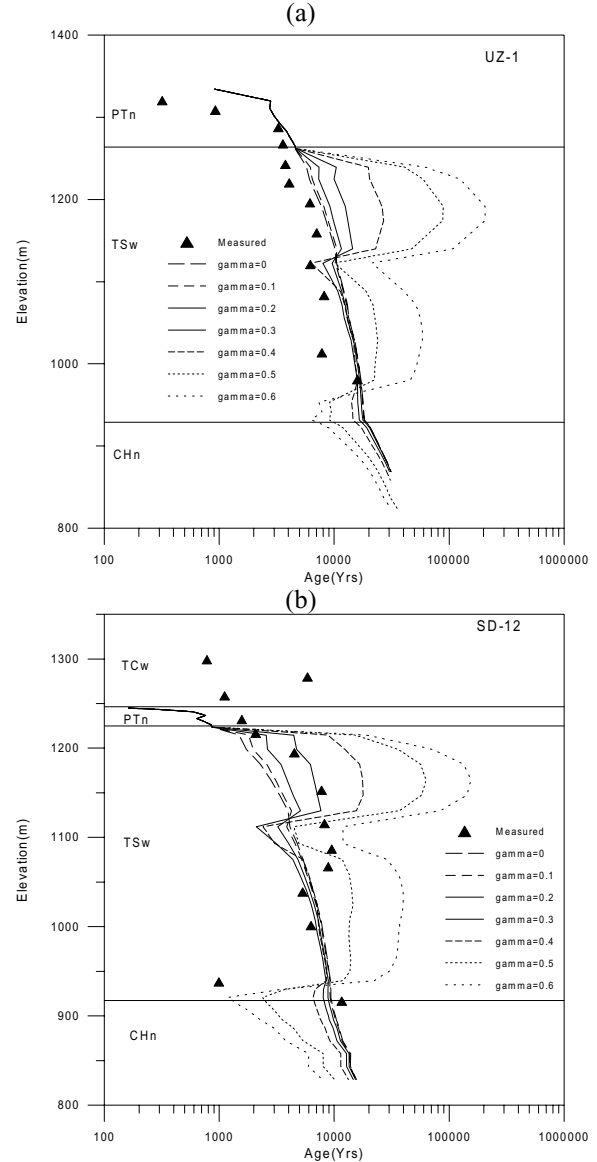


Figure 3. Comparisons between simulated water travel times (ages) for rock matrix at boreholes (a) USW UZ-1 and (b) USW SD-12 and the corresponding Carbon-14 ages (Yang, 2002) for several γ values.

Fig. 3 shows simulated water travel times (ages) for different γ values of the TSw formation. Note that a major path for tracer transport into the tuff matrix is from fractures to the tuff matrix, which is different from tracer transport processes within a single continuum. The considerable sensitivity of simulated results to γ indicates that carbon-14 data are useful for validating the AFM and for constraining the γ

values for the TSw unit. For γ values ranging from 0.2 to 0.4, simulated results approximately match the observations for the two boreholes simultaneously, although a better match is obtained for USW SD-12 than that for USW UZ-14 (as a result of subsurface heterogeneity). In our current model, the heterogeneity within each geological layer is not considered. A larger γ value generally corresponds to a larger travel time (for the matrix), because of the smaller degree of matrix diffusion resulting from a smaller fracture-matrix interfacial area available for mass transport between fractures and the matrix. Note that the observed carbon-14 ages and simulated water travel times result from a combination of solute transport in fractures and the relatively slow matrix diffusion process. The spatial variability of the degree of matrix diffusion is the reason why the simulated water travel times and the observed ages in Fig. 3 are not always monotonically increasing with depth in the TSw.

A sharp change in simulated water travel times occurs at an elevation of about 1,100 m for two boreholes (Fig. 3). This is because the upper portion of the TSw unit has relatively small fracture density values and therefore corresponds to a smaller degree of matrix diffusion for a given γ value. For the borehole USW UZ-1, simulated water travel time is generally longer than the observation for a given elevation. This may be owing to a subsurface heterogeneity that gives larger fracture densities (resulting in a larger degree of matrix diffusion) at the borehole location than what are used in the numerical model. Layer-averaged fracture properties are used in the site-scale model of the unsaturated zone of Yucca Mountain. In general, a comparison between simulated water travel times and observed carbon-14 ages indicates that the AFM with γ values for the TSw between 0.2 and 0.4 can reasonably represent the data.

To check the consistency of the AFM with the coating data, a one-dimensional model for borehole USW SD-12 is used. The model is the same as that described above. USW SD-12 is chosen because it is located near the middle of the underground tunnel where coating data were collected. Two infiltration rates (Flint et al., 1996), present day mean infiltration rate (3.4 mm/yr) and glacial maximum infiltration rate (17.3 mm/yr), are used for simulations. Again, uniform γ distributions for the TSw formation are employed. The latter infiltration rate is about five times as large as the former rate and represents the maximum infiltration rate in past climates.

Fig. 4 shows the simulated average portion of active fractures, f_a , for the TSw formation as a function of infiltration rate and γ . The average portion is calculated from Eq. (1) using the average effective saturation for the TSw formation. The calculated f_a values are about 10 % to 40% for γ values ranging from 0.4 to 0.2 that are similar to those used for matching the carbon-14 data. Recall that the estimate of the active fracture portion from fracture coating data in the TSw was about 10%. Note that not all the active flow paths are associated with coatings and that coatings can also disappear due to dissolution. For example, Wang et al. (1999) found a flow feature under ambient conditions from the unsaturated zone of Yucca Mountain. This flow feature does not have coatings. Therefore, coated fractures may represent the lower limit of the number of active fractures at the Yucca Mountain site. Since the number of active fractures increases with γ , $\gamma = 0.4$ may roughly represent the upper limit for the actual γ values. For γ values less than 0.4, the calculated f_a values do not change significantly for the two infiltration rates (Figure 4), which is consistent with the observation of the stability of flow paths over time.

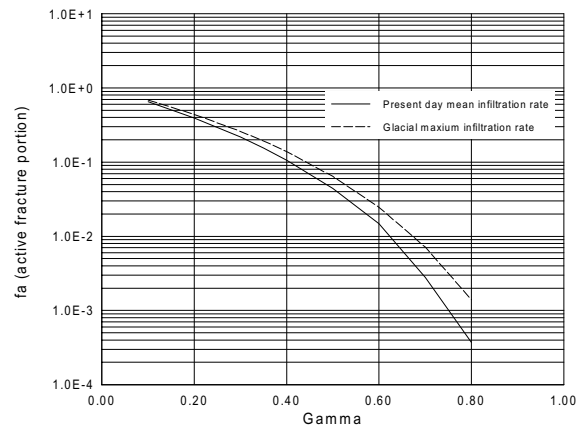


Figure 4. Simulated average portion of active fracture for the TSw formation as a function of infiltration rate and γ .

In summary, we have shown in this section that the AFM-based simulation results for $\gamma = 0.2 - 0.4$ approximately match the observed carbon-14 age data for the two borehole simultaneously. The similar range of γ value results in f_a values consistent with the portion of active fracture (10%) estimated from the fracture coating data. The insensitivity of f_a values for $\gamma = 0.2 - 0.4$ to infiltration rates is also consistent with the stability of flow paths over time that were observed from the unsaturated zone of Yucca Mountain. All of these observations support the validity of the AFM.

CONCLUDING REMARKS

Accurately modeling flow and transport processes in natural unsaturated systems is very difficult, largely because these processes are generally localized and associated with fingering and preferential flow paths. While the continuum approach is still the most feasible choice for many large-scale problems encountered in the real world, the traditional continuum approach has generally failed in capturing localized flow behavior, because of the use of volume averaging at a subgrid scale.

Two schools of thought exist regarding how to address the problem mentioned above. A number of researchers suggest using modeling approaches that are completely different from the continuum approach, such as the DLA and percolation-based approaches (e.g., Ewing and Berkowitz, 2001; Glass 1993; Flury and Flühler 1995). These approaches have been successfully used to represent relatively small-scale observations. However, the use of these discrete approaches is very limited for large-scale applications. Furthermore, completely satisfactory theories underlying these approaches are still missing, and some critical steps in these approaches are somewhat arbitrary (Meakin and Tolman, 1989; Ewing and Berkowitz, 2001).

The other school of thought is to modify the continuum approach by incorporating key features of the discrete approaches (or small-scale observations), considering that the continuum approach is computationally efficient and robust, and often preferred for large-scale problems. Obviously, the AFM is a product of this school of thought. Note that although these discrete approaches have different physical origins, they are connected by the same class of flow patterns: fractals. Fractal flow behavior is also supported by field observations from different unsaturated systems, including the unsaturated zone of Yucca Mountain. Because of the relative simplicity of fractal-based characterizations, we believe that the key small-scale features in unsaturated systems can be successfully incorporated into large-scale continuum approaches. This is partially supported by the consistency between simulation results based on the AFM and a variety of field observations from the unsaturated zone of Yucca Mountain.

While we have demonstrated that the AFM is, in general, consistent with fractal flow behavior and can capture the major flow and transport features in the unsaturated zone of Yucca Mountain, more studies are needed to further improve it. For example, the AFM assumes a homogeneous distribution of flow field within the active-fracture continuum, whereas in reality the flow field may be very heterogeneous. One way to resolve this issue may be based on the concept

of the multifractal (e.g., Feder 1988; Liu and Molz 1997).

ACKNOWLEDGMENT

We are indebted to Q. Zhou at Lawrence Berkeley National Laboratory for his careful review of a preliminary version of this manuscript. This work was supported by the Director, Office of Civilian Radioactive Waste Management, U.S. Department of Energy, through Memorandum Purchase Order EA9013MC5X between Bechtel SAIC Company, LLC, and the Ernest Orlando Lawrence Berkeley National Laboratory (Berkeley Lab). The support is provided to Berkeley Lab through the U.S. Department of Energy Contract No. DE-AC03-76SF00098.

REFERENCES

- Bodvarsson, G. S., and Y. Tsang, (Guest Editors), Yucca Mountain Project, *J. Contam. Hydrol.* 38,1-146, 1999.
- Bodvarsson, G.S., H.H. Liu, R. Ahlers, Y.S. Wu and E. Sonnenthal, Parameterization and upscaling in modeling flow and transport at Yucca Mountain, in *Conceptual Models of Unsaturated Flow in Fractured Rocks*, National Academy Press, Washington, D.C., 2000.
- Ewing, R. P. and B. Berkowitz, Stochastic pore-scale growth models of DNAPL migration in porous media, *Advances in Water Resources* 24, 309-323, 2001.
- Fabryka-Martin J., A. Meijer, B. Marshall, L. Neymark, J. Paces, J. Whelan and A. Yang, *Analysis of geochemical data for the unsaturated zone*. Rep. ANL-NBS-HS-000017. CRWMS M&O, Las Vegas, Nevada, 2000.
- Feder J., *Fractals*. Plenum Press, New York, 1988.
- Flint, A.L., J. A. Hevesi, E.L. Flint, *Conceptual and numerical model of infiltration for the Yucca Mountain area, Nevada*, Water Resources Investigation Report-96. U.S. Geologic Survey, Denver, Co., 1996.
- Flury M. and H. Flühler, Modeling solute leaching in soils by diffusion-limited aggregation: Basic concepts and applications to conservative solutes, *Water Resour. Res.* 31, 2443-2452, 1995.
- Glass R.J., Modeling Gravity-Driven fingering using modified percolation theory, In *Proceedings of the fourth annual international conference on high level radioactive waste conference*, Las Vegas, Nevada, 1993.

- Glass, R. J., M. J., Nicholl, and V. C., Tidwell, Challenging and improving conceptual models for isothermal flow in unsaturated, fractured rocks through exploration of small-scale processes. Rep. SAND95-1824, Sandia National Laboratories, Albuquerque, NM, 1996.
- Liu, H. H. and F.J. Molz, Multifractal analyses of hydraulic conductivity distribution, *Water Resour. Res.* 33, 2483-2488, 1997.
- Liu, H. H., C. Doughty, and G. S. Bodvarsson, An active fracture model for unsaturated flow and transport in fractured rocks, *Water Resour. Res.* 34, 2633-2646, 1998.
- Liu, H.H., and C.F. Ahlers, Calibrated properties model. Rep. MDL-NBS-HS-000003. BSC, Las Vegas, Nevada, 2003.
- Mandelbrot B. B., *The fractal geometry of nature*, W.H. Freeman, New York, 1982.
- Meakin P. and S. Tolman, Diffusion-limited aggregation, In *Fractals in the natural sciences*. Princeton Univ. Press, Princeton, N.J., 1989.
- Paces, J. B., L.A. Newmark, B.D. Marshall, J.F. Whelan, and Z.E. Peterman, Ages and origins of subsurface secondary minerals in the Exploratory Studies Facility, Milestone Rep. 3GQH450M. U. S. Geol. Surv., Denver, Co, 1996.
- Persson M., H. Yasuda, J. Albergel, R. Berndtsson, P. Zante, S. Nasri, and P. Ohrstrom, Modeling plot scale dye penetration by a diffusion limited aggregation (DLA) model, *J. Hydrol.* 250, 98-105, 2001.
- Pruess, K., TOUGH2-A general purpose numerical simulator for multiphase fluid and heat flow, Rep. LBNL-29400. Lawrence Berkeley National Laboratory, Berkeley, CA, 1991.
- Pruess, K., B. Faybishenko, and G.S. Bodvarsson, Alternative concepts and approaches for modeling flow and transport in thick unsaturated zones of fractured rocks, *J. Contam. Hydrol.*, 38, 281-322, 1999.
- Smith J.E. and Z. F. Zhang, Determining effective interfacial tension and predicting finger spacing for DNAPL penetration into water-saturated porous media, *J. Contam. Hydrol.* 48, 167-183, 2001.
- Stauffer D. and Aharony, A., *Introduction to Percolation Theory*, Tayler & Francis, 1991.
- Su, G.W., J.T. Geller, K. Pruess, and F. Wen, Experimental studies of water seepage and intermittent flow in unsaturated rough-walled fractures, *Water Resour. Res.*, 35, 1019-1037, 1999.
- van Genuchten, M., A closed-form equation for predicting the hydraulic conductivity of unsaturated soil, *Soil Sci. Soc. Amer. J.*, 44, 892-898, 1980.
- Wang J.S.Y., R.C. Trautz, P.J. Cook, S. Finsterle, A.L. James and J. Birkholzer, Field tests and model analyses of seepage into drift. *J. Contam. Hydrol.*, 38, 232-347, 1999.
- Witten, T.A. and L. M. Sander, Diffusion-limited aggregation: A kinetic critical phenomenon, *Phys. Rev. Lett.* 47, 1400-1403, 1981.
- Wilkinson D. and J.F. Willewsen, Invasion percolation: A new form of percolation theory, *J. Phys. A.* 16, 3365-3376, 1983.
- Wu, Y. S., C.F. Ahlers, P. Fraser, A. Simmons, K. Pruess, *Software qualification of selected TOUGH2 modules*, LBNL-39490, Lawrence Berkeley National Laboratory, Berkeley, CA., 1996.
- Yang, I.C. 2002, Percolation flux and transport velocity in the unsaturated zone, Yucca Mountain, Nevada, *Applied Geochemistry*, 17, 807-817, 2002.